Science of the Total Environment 970 (2025) 179015

Contents lists available at ScienceDirect

Science of the Total Environment

journal homepage: www.elsevier.com/locate/scitotenv

Baseflow CO_2 fluxes in small tropical rivers driven by hydrological dynamics

Daniela Vasconcelos Machado [a,b,*], Eduardo Duarte Marques [c], Andréa da Consolação de Oliveira Carvalho [d], Eduardo Paim Viglio [e], Everton Assunção Martins dos Santos [c], Rozane Valente Marins [d], Gerson Cardoso da Silva Júnior [b], Emmanoel Vieira Silva-Filho [a]

[a] Fluminense Federal University (UFF). Niteroi, Post-Graduate Program in Geosciences (Environmental Geochemistry), Chemistry Institute, RJ, Brazil
[b] Federal University of Rio de Janeiro (UFRJ), Post-Graduate Program in Geology, Geosciences Institute, Rio de Janeiro, RJ, Brazil
[c] Geological Survey of Brazil (SGB/CPRM), Belo Horizonte Regional Office, Belo Horizonte, MG, Brazil
[d] Federal University of Ceará, Marine Science Institute/LABOMAR, Av. da Abolição, 3207, 60, 165-081 Fortaleza, CE, Brazil
[e] Geological Survey of Brazil (SGB/CPRM), Rio de Janeiro Office, Rio de Janeiro, Brazil.

HIGHLIGHTS

- Upper São Francisco Basin rivers emit approximately 1.56 Pg C yr^{-1}, with 95 % confidence interval. (84)
- pCO_2 corrected values are up to 15 times lower than pCO_2 calculated from pH-TA. (80)
- Bed friction dissipation controls turbulence in 85 % of rivers analyzed. (72)
- k_{600} parameterization reveals high spatial variability, slope's strong influence. (82)
- First CO_2 emission estimates for the Upper São Francisco Basin, Brazil. (73)

GRAPHICAL ABSTRACT

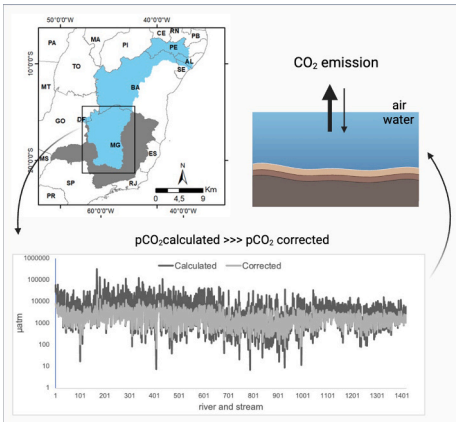

ARTICLE INFO

Editor: Wei Ouyang

Keywords:
CO_2 partial pressure
CO_2 fluxes water-air

ABSTRACT

Dry season CO_2 fluxes were estimated for 1418 small rivers and streams in the Upper São Francisco Basin (USFB), Brazil. This first basin-scale estimate revealed a substantial contribution of 1.52 Pg C yr^{-1} (95 % confidence interval: 1.40 to 1.64 Pg C yr^{-1}). pCO_2 values, calculated from pH and total alkalinity (TA) and subsequently corrected, ranged from 66 to 20,200 µatm (2191 ± 1791 µatm; coefficient of variation of 82 %). Approximately

* Corresponding author: at: Av. Athos da Silveira Ramos, 274 - UFRJ – CCMN – IGEO – Departamento de Geologia - Bloco G, Secretaria do PPGL, sala G1-03, Campus Ilha do Fundão (Cidade Universitária) - CEP: 21.941-916, Rio de Janeiro, RJ, Brazil.
E-mail addresses: dvasconcelos@id.uff.br (D.V. Machado), eduardo.marques@cprm.gov.br (E.D. Marques), andreadaconsolacao@gmail.com (A.C.O. Carvalho), eduardo.viglio@sgb.gov.br (E.P. Viglio), everton.santos@sgb.gov.br (E.A.M. dos Santos), rmarins@ufc.br (R.V. Marins), gerson@geologia.ufrj.br (G.C. da Silva Júnior), emmanoelvieirasilvafilho@id.uff.br (E.V. Silva-Filho).

https://doi.org/10.1016/j.scitotenv.2025.179015
Received 15 November 2024; Received in revised form 25 February 2025; Accepted 26 February 2025
Available online 5 March 2025

Gas transfer velocity
Energy dissipation
Climate change

95 % of rivers exhibited evasive fluxes with bed friction dissipation as the dominant control on turbulence in over 85 %. Analysis of gas transfer velocity (k_{600}) parameterizations revealed significant inter-equation differences, high spatial variability, and strong slope influence. These findings highlight the potentially role of small tropical rivers and streams in global carbon cycling and provide the first CO_2 emission estimate for the USFB.

1. Introduction

As a consequence of the CO_2 concentration imbalance, climate change has already surpassed planetary boundaries established as safe for Earth's resilience (Rockström et al., 2009; Wang-Erlandsson et al., 2022). These changes have resulted in significant impacts on local and regional climates (Joshi and Siddaiah, 2021). Consequently, the Intergovernmental Panel on Climate Change (IPCC) acknowledged that a 2 °C increase above pre-industrial levels would already result in adverse effects on the natural environment, human health, and well-being. In light of this, the IPCC proposed that global warming should not exceed 1.5 °C above the Industrial Era (Canadell et al., 2021). A current challenge is to identify and quantify reservoirs that serve as sources and sinks of CO_2 in the environment in order to aid in mitigating and managing global warming (Liu et al., 2022).

The flux of CO_2 through the water-atmosphere interface (CO_2 evasion) from inland waters (lakes, rivers, streams, and reservoirs) plays a significant role in the global carbon cycle (Keller et al., 2020). The estimation of CO_2 evasion in global inland waters ranges from 1.40 to 3.28 Pg C yr^{-1}, indicating that this environment are supersaturated in partial pressure of carbon dioxide (pCO_2) when compared to the atmosphere (Wen et al., 2021).

Global riverine CO_2 emissions are estimated between 0.2 and 2.2 Pg C yr^{-1}, and suggest that tropical ecosystems exhibiting substantially higher emissions than temperate, boreal, and arctic zones (Liu et al., 2022; Raymond et al., 2013; Tang et al., 2023; Wen et al., 2021). Small rivers and streams are recognized as key contributors to this CO_2 efflux, with tropical regions identified as hotspots, potentially accounting for up to 57 % of global inland water emissions (Liu et al., 2022; Quick et al., 2019). However, significant uncertainties remain regarding carbon emissions from these smaller systems, particularly in tropical regions like Brazil (Machado et al., 2023) representing a potential blind spot in global carbon cycle estimates (Marx et al., 2017; Tang et al., 2023).

Despite advances in estimating riverine carbon fluxes, significant uncertainties remain, primarily due to spatial and temporal variability in gas transfer rates and limitations in sampling frequency and coverage. These uncertainties are exacerbated discrepancies between different k_{600} parameterizations and challenges in resolving spatial heterogeneity in gas transfer across diverse river systems (Raymond et al., 2012; Ulseth et al., 2019).

In this context this study aimed to estimate the contribution of CO_2 degassing from the Upper São Francisco Basin, a tropical watershed in Brazil. The estimation of the basin was based on the analysis of 1418 rivers and streams. The challenges associated with estimating fluxes were discussed. The following investigations were conducted: (i) the modeled pCO_2 was corrected and evaluated; (ii) the spatial variability of the k_{600} was investigated using different parameterizations; finally (iii) the CO_2 fluxes of the watershed were estimated by analyzing the small rivers and streams that were spatially distributed within the basin.

2. Study area

The research was conducted in the Upper São Francisco Basin, which corresponds to 37 % (233,564 km^2) of the total of the São Francisco River Basin (BHSF) (catchment area 639,219 km^2) (Fig. S1 in Supplementary Material). The BHSF is one of the main watersheds in Brazil, with high mining and agricultural activity, as well as a rich biodiversity.

The Upper São Francisco Basin is situated within a tropical climate, characterized by mild temperatures and high annual precipitation in the region proximate to the headwaters, which gradually transitions to higher temperatures and lower precipitation in the drought polygon region (arid region in Brazil). The average temperature is 23 °C, with the average annual precipitation varying from 1000 to 2000 mm. The São Francisco River (main channel) extends for 2863 km from the Serra da Canastra (headwater region, SE) to the Atlantic Ocean (estuary, NE).

The region encompasses the convergence of three important Brazilian biomes (Atlantic Forest, Cerrado, and Caatinga) and the country's largest karst region. The basin is subject to intense anthropogenic activities, with the presence of an important metallogenic region (Quadrilátero Ferrífero). This region is primarily involved in mineral extraction, with iron and manganese being the most prominent minerals extracted. The region is home to approximately 8 million people, with water usage is allocated for human consumption, industrial purposes, and agriculture (FJP, 2019).

The basin drains different lithologies from the pre-Cambrian to the Phanerozoic age. The most prevalent lithotypes in the basin are limestone, metapelite rocks (Bambuí Group), and sandstones (Urucuia and Areado Groups). The Bambuí Group, which form part of the Paraopeba Supergroup, and is distinguished by the prevalence of carbonate lithologies in the region. The limestones of the Lagoa do Jacaré and Serra de Santa Helena formations, as well as the dolomites of the Sete Lagoas Formation, are the dominant lithologies in the study area.

3. Materials and methods

3.1. Database

This study was conducted using the database owned by the Geological Survey of Brazil (SGB), containing samples (1418 samples) of surface water at the small rivers and streams. Fieldwork campaigns occurred from 2008 to 2010, in dry season (from April to October), corresponding to the base flow. The database contains, for each sample, value of the physicochemical and hydraulic parameters. The methods and protocols are described in detail below.

Surfaces water samples were collected at the mouths of small rivers and streams (predominantly with a drainage area < 500 km^2). The SGB adopts a systematic approach to hydrogeochemical mapping, utilizing regional sample distribution to cover a maximum area and obtain higher resolution in the results (Marques et al., 2023). The collection site was previously spatialized and, corrected in the fieldwork whether necessary. The samples were collected in sterilized and clean polyethylene bottles (1000 mL).

The total alkalinity aliquots remained "in natura". The aliquots were stored in polyethylene tubes and kept refrigerated until analysis at the Análises Minerais Laboratory (LAMIN) of the Geological Survey of Brazil (SBG/CPRM), immediately after collection. The concentrations (TA in $mgCaCO_3L^{-1}$ and converted in mM) was determinate by the analytical procedure for determining alkalinity by carbonate/bicarbonate and the acid titration analytical method, using the Metrohm 905 Titrando automatic titrator. TA accuracy is 1.8 $mgCaCO_3L^{-1}$.

After collecting the water samples, pH, temperature (T °C), electric conductivity (EC μS cm^{-1}) and dissolved oxygen (expressed in O_2sat%) were instantly measured *in situ* using portable measuring equipment (model OAKTIB OCD 650), prior calibrated. The specifications of the equipment reported pH accuracy ±0.002, temperature accuracy ±0.5 °C, conductivity accuracy ±1 % and dissolved oxygen accuracy ±2 %.

3.2. Hydraulic parameters

Discharge (Q in $m^3\ s^{-1}$) of each microbasin was obtained from its relationship with the water surface area (A in km^2) (Tucci, 2001) and discharge data for the sampling period were obtained from the HIDROWEB database, belonging to the National Water and Basic Sanitation Agency (Agência Nacional de Águas e Saneamento Básico, ANA - Brazil). Subsequently, a relationship was generated between the discharge found in the fluviometric stations and their respective drainage areas, allowing an adjustment line as a power function, with generally Eq. 1 by:

$$Q_{fs} = aA_{fs}{}^{b} \quad (1)$$

where a and b correspond to the coefficients determined by the least squares method, Q_{fs} is the discharge of the fluviometric stations and A_{fs} is equal to drainage area of the fluviometric stations. Ten equations of the power function were generated, one for each sector of the study basin. Using microbasin area, it was possible to measure the discharge of each microbasin. This methodology becomes possible since each analyzed microbasin constituted a homogeneous region in terms of hydrology, geology, soil, relief, and climate characteristics.

The current velocity (V in m s^{-1}) of the each microbasin was estimated from the hydraulic geometry theory, which makes it possible to relate it to discharge (Q) (Leopold and Maddock, 1953). In this study, the Eq. 2 proposed by Raymond et al. (2012) was used. The depth (D, meters) and width (W, meters) of the rivers were measured *in situ*. Microbasins where it was not possible to measure these parameters *in situ* (D < 6 % and W < 2 % of the total microbasins), they were estimated using the hydraulic Eqs. 3 and 4, respective. (Raymond et al., 2012). Drainage area (A, km^2), elevation (E, meters) and slope (S, unitless) were measured by geoprocessing procedures using the ArcGis (version 10.8.1).

$$\ln V = 0.285 \ln Q - 1.64 \quad (2)$$

$$\ln D = 0.294 \ln Q - 0.895 \quad (3)$$

$$\ln W = 0.423 \ln Q + 2.56 \quad (4)$$

3.3. CO_2 partial pressure

The CO_2 partial pressure of the water (pCO_{2w}, μatm) was estimated by the indirect method, which is made from measurements of at least two of the parameters belonging to the carbonate system. In this study was used the pH - TA pair. To perform the estimate was used the free software CO2Calc v4.0.9 (Robbins et al., 2010), which is an extension of the CO2SYS (Lewis et al., 1998).

The input settings used in the program were the most recommended and appropriate for freshwater, using pH, Total Alkalinity (TA, μM), temperature (°C) and silicium (Si, μM). In this work was used the NBS pH scale, the carbonic acid dissolution constants (k_1 and k_2) (Millero, 1979), the dissociation constant of sulfate ($KHSO_4$) (Dickson, 1990), and the dissolution constant of borate (total boron) (Lee et al., 2000). The error propagation of the pCO_2 calculation made using the pH-TA pair was calculated (Orr et al., 2018).

The utilization of the carbonic equilibrium to estimate the concentration of CO_2 is not a novel methodology (Millero, 1995; Millero, 1979; Neal et al., 1998). However, the use of this methodology in river systems has been discussed in recent literature (Abril et al., 2015; Hunt et al., 2011; Liu et al., 2020; Ran et al., 2017), in particular the use of the pH-TA pair. Hunt et al. (2011) demonstrated that pCO_2 values calculated by CO2Calc exhibited <2 % discrepancy compared to pCO_2 values computed using PHREEQC (Parkhurst and Appelo, 1999). Ran et al. (2017) reported that pCO_2 values estimated by the pH-TA pair showed no significant difference (< 8 % difference) from pCO_2 values obtained through the headspace equilibration method. However, inaccuracy in pH and TA measurements can result in cumulative uncertainties in pCO_2 estimates, due to ionic strength and organic alkalinity, respectively.

Regarding pH measurements, the poor performance of the commercial electrodes in low ionic strength freshwaters results in a measurement error biased toward lower values, rendering the measurements unreliable (Liu et al., 2020). Therefore, before calculating pCO_2 in CO2Calc program, the pH values were corrected using the Eq. 5–7 for flowing condition (Liu et al., 2020):

$$pH_{corrected} = pH_{measured} - \Delta pH \quad (5)$$

$$\Delta pH = 0.06 + 0.08\ log_{10}\ (I) \quad (6)$$

$$I = 1.3\ 10^{-5}\ EC\ (\mu S\ cm^{-1}) \quad (7)$$

Where $pH_{measured}$ is o pH measured *in situ*; ΔpH is the estimate pH measurement error from ionic strength (I) for flowing condition.

Another concern is about the total alkalinity values. Discussions suggest an overestimation generated during modeling due mainly to organic alkalinity (for instance, buffering capacity from organic anions), and consequently in the buffering capacity of the river, especially in freshwater with acidic pH and total alkalinity below 1000 μmol L^{-1} (Abril et al., 2015; Wang et al., 2021). However, correcting total alkalinity values to reduce the effect of organic alkalinity did not demonstrate effectiveness in CO_2 concentration calculations when compared to direct measurements (Abril et al., 2015; Liu et al., 2020). On the other hand, the influence of organic alkalinity can generate an overestimate ranging from 50 to 300 % in relation to measurements (*in situ* pCO_2) (Abril et al., 2015).

From these discussions, attempts to correct the calculated pCO_2 values have been proposed by Tang et al. (2023). In order to obtain a better estimate for pCO_2 values and fluxes of the CO_2 for the Upper São Francisco Basin, the calculated pCO_2 values was corrected using the Eq. 8 ($R^2 = 0.73$, $p < 0.001$, sample size = 31) reported for dry season, with pCO_2 values in μatm (Tang et al., 2023).

$$pCO_{2corrected} = 23.5\ e^{1.2288 log pCO_{2calculed}} \quad (8)$$

3.4. Energy dissipation rate

The gas transfer can be affected for both turbulence from (i) depth-scale form drag (ε_d), that correspond for turbulent energy dissipation rate due wind-forced processes and is based on stream power per unit weight of water near the free surface (Moog and Jirka, 1999), (ii) and bed friction (ε_s) for smooth or small-roughness flows (Zappa et al., 2007). The dissipation rate varied on the extremes of pure bed friction (ε_s) and pure depth-scale form drag (ε_d), where generally, system river generally reflects this both turbulence processes. This classic concept is explaining in the model describe by (Moog and Jirka, 1999).

The energy dissipation rate were calculated by Eqs. 9 and 10 (Moog and Jirka, 1999; Raymond et al., 2012), where ε_d is the dissipation depth-scale form drag ($m^2\ s^{-3}$) and, ε_s correspond dissipation rate due to bed friction ($m^2\ s^{-3}$) and, u_* = friction velocity; R_h = hydraulic radius; g = acceleration due to gravity (9.81 m s^{-2}); S = slope (unitless); V = current velocity (m s^{-1}); D = depth (m) and W = width (m).

$$\varepsilon_d = gSV \quad (9)$$

$$\varepsilon_s = u_*^3/D \quad (10)$$

$$u_* = (gR_hS)^{0.5}$$

$$R_h = DW/(W + 2D)$$

3.5. Water-air CO_2 fluxes

The CO_2 gas exchange that occurs between the water-atmosphere

interface is evaluated by the vertical flux FCO_2 that corresponds to the water – atmosphere interface CO_2 flux (mmol m^{-2} d^{-1}) and can be estimated by the theoretical diffusion model, by Eq. 11 (Liss and Slater, 1974):

$$FCO_2 = k_{CO_2} KH \Delta pCO_2 \quad (11)$$

Where the ΔpCO_2 is the difference between the CO_2 partial pressure of the water (pCO_{2w}) and CO_2 partial pressure of the atmosphere in equilibrium of the water surface (pCO_{2air}), both in μatm. The pCO_{2air} can be considered stable when compared to pCO_{2w}. In this work, for the pCO_{2air} was used the concentration monitored by the Mauna Loa Observatory. The current value of reference ranges from 400 to 420 μatm (Li et al., 2018). However, as the samples were not collected in currently date, the value of reference was used following the respective years of collection. The pCO_{2air} values between 2008 and 2010 vary from 383 to 393 μatm (Fig. S2 in Supplementary Material). This open data was obtained from the National Oceanic and Atmospheric Administration (NOAA) website. The CO_2 solubility (KH, mmol m^{-3} μatm^{-1}) was calculated according to the (Weiss, 1974) Eq. 12, using the temperature in Kelvin (K).

$$kH = e^{(-58{,}0931+90{,}5069\ (100/T)+22{,}2940 ln(T/100))} \quad (12)$$

The k_{CO_2} correspond CO_2 gas transfer rate (m d^{-1}) between the water-atmosphere interface. This factor is a difficult parameter to estimate. It depends on rate flow and corresponds to a given coefficient as a function of turbulence, water viscosity (v) and gas molecular coefficient (D). In this study, k_{CO_2} was calculated based on the empirical model using a Schmidt number (*Sc*) and, k_{600} approach following the Equations from 13 to 16.

$$Sc_{CO_2} = 1911.1 - 118.11\ T + 3.4527\ T^2 - 0.04132\ T^3 \quad (13)$$

$$k = Sc^{-n} \quad (14)$$

$$k_1/k_2 = (Sc_1/Sc_2)^{-n} \quad (15)$$

$$k_{CO_2} = k_{600}\ (Sc_{CO_2}/Sc_{600})^{-0.5} \quad (16)$$

Where: Sc_{600} = 600; for CO_2 gas in freshwater (T = 20 °C).

The Schmidt number correspond the ratio between water viscosity and gas molecular coefficient (v/D) and is obtained as a function of the temperature (°C) of the water, where the constant is specific to each gas (for CO_2 gas see Eq. 13) (Wanninkhof, 1992). It can be correlated with the gas transfer rate by the Eq. 14, where *n* corresponds to the Schmidt number exponent that is usually given as values of 0.5 for the river system and 0.7 for open ocean. It is possible to estimate a gas transfer velocity of a given gas (k_1) from another gas (k_2), using your correlated with *Sc* through the ratio of the gas transfer velocity (k_1/k_2), as the Eq. 15. A common approach is to estimate the velocity of k_{CO_2} correlating with the k_{600}, that is a temperature-normalized gas transfer velocity value, where for a temperature equal to 20 °C for CO_2 gas in freshwater, the Schmidt number is 600 (Sc_{600}) (Jähne et al., 1987). Therefore, it is possible to find k_{CO_2} from the k_{600} by the Eq. 16. The Sc_{CO_2} corresponds to the Schmidt number for CO_2 in relation to the river temperature measured *in situ* (Raymond et al., 2012). The k_{600} (m d^{-1}) is obtained as a parameterization of the hydraulic parameter (Raymond et al., 2012) and wind velocity (*e.g.* Wanninkhof, 1992).

Many studies have demonstrated that for small rivers and streams the parameterization of k_{600} is better modeled using the hydraulic parameters instead of the wind speed (Alin et al., 2011; Raymond et al., 2012). Thus, from the review of many parameterizations, in this work was applied 6 equations using current velocity (V) of the water, water depth (D) and stream slope (S) (Table 1).

3.6. Data analysis

Data statistics were evaluated using the software Statistica (StatSoft, version 14) and the program RStudio (RStudio Team, 2022) in the R core environment (R core team, 2022). The percentiles 25 % (25th) and 75 % (75th) were calculated (Table S1 in Supplementary Material). Spatial distribution analysis was performed by ArcGIS (Version 10.8.1). Graphs were created using GrapherTM (Golden Software, LLC). The data were checked for normality using the Kolmogorov-Smirnov test and the results showed that the data were not normally distributed. Outlier were identified using the Robust Regression Outlier removal, ROUT test (Q = 1 %), which is an extension of the Grubbs test and indicated for non-parametric data. Mann-Whitney test and Kruskal-Wallis test, non-parametric test, were used to evaluate significant differences between the parameters pH, pCO_2, k_{600} and FCO_2. Spearman correlation analysis was employed to detect relationships between parameters.

Table 1
Fitted equations for predicting the k_{600} based on current velocity (V, m s^{-1}), depth (D, m), stream slope (S, unitless), Froude number (Fr = V/(gD)$^{0.5}$), energy dissipation (ε_d = gSV, m^2 s^{-3}), acceleration due to gravity (g = 9.81 m s^{-2}). For the Eq.6: a = ε_d < 0.02, b = ε_d > 0.02. Eq.1 to Eq.5 by (Raymond et al., 2012) and Eq.6 by (Ulseth et al., 2019).

	Equation
Eq.1	k_{600} (m d^{-1}) = $(VS)^{0.89}$ $D^{0.54}$ 5037
Eq.2	k_{600} (m d^{-1}) = 5937 (1–2.54 Fr^2) ($VS^{0.89}$) $D^{0.58}$
Eq.3	k_{600} (m d^{-1}) = 1162 $S^{0.77}$ $V^{0.85}$
Eq.4	k_{600} (m d^{-1}) = $(VS)^{0.76}$ 951.5
Eq.5	k_{600} (m d^{-1}) = VS 2841 + 2.02
Eq.6	ln[k_{600}] (m d^{-1}) = 3.10 + 0.35 ln[εd]^a ln[k_{600}] (m d^{-1}) = 6.43 + 1.18 ln[εd]^b

4. Results

4.1. Hydraulic parameters

Hydraulic parameters (area [A], elevation [E], slope [S], velocity [V], width [W], and depth [D]) are summarized in box plots in the Supplementary Material (Fig. S3). Catchment size ranged from 2 to 1129 km^2 (CV: 78 %), with 99 % of catchments ≤500 km^2 and percentiles of 25th = 60 km^2; median = 112 km^2, and 75th = 171 km^2. Topographic amplitude (E) varied from 338 to 1644 m (range = 1306; CV: 32 %). Most of the microbasins are located below 1000 m (75th = 717 m). The southern region has exhibited higher elevations compared to the northern region. Slope (S) ranged from 0.002 to 0.12 (CV: 52 %), with 75 % of slopes <0.03 and ~ 60 % > 0.04 (4 %). Lower slopes were predominantly found in the northern region, while the eastern region, corresponding to microbasins originating in the orogenic belt, exhibited the largest slopes. Current velocity (V) ranged from 0.01 to 0.30 m s^{-1} (0.15 ± 0.06 m s^{-1}). Microbasins near the karst region had lower current velocities, showing a moderate positive correlation with microbasin area (ρ = 0.53, p < 0.05).

In general, the microbasins has an average channel width (W) <10 m (about 72 % of the rivers), with 25th = 3.5 m, 75th = 12 m and a maximum of 850 m. Width is a prominent parameter in the differences between microbasins, evidenced by the high C.V.: 346 %, with median = 50th = 6 m and mean = 17 ± 59 m. Microbasins larger than 20 m are sporadically encountered in specific points, appearing as outliers (144 samples). Rivers and streams were generally shallow, with an average depth (D) of 1.2 ± 1.1 m, and 75th < 1.5 m. 93 % of the rivers and streams are shallower than 3.0 m. Deeper rivers were occasionally found, primarily in the northern sector, with a maximum depth of 10 m, and D > 3.0 m are identified as outliers (99 samples).

4.2. Physicochemical parameters

The physicochemical parameters exhibited a non-normal distribution according to the Kolmogorov-Smirnov test. The box plot can be found in the Supplementary Material (Fig. S4). Temperature (T) and

oxygen saturation (O_2Sat%) did not appear to be outliers according to the ROUT test (Q = 1 %). The temperature range was 14.6 to 35.0 °C, with an average of 23.4 ± 3.0 °C. There was low spatial variability (C.V.: 13 %). The O_2Sat% exhibited an average of 68 ± 21 %, with a range of 1 to 157 % (75th = 82 %; C.V.: 31 %). This represents the value of the dissolved oxygen (DO) between 0.05 and 12.4 mg L^{-1}. In aquatic environment it is defined that DO below 5.0 mg L^{-1} suggests DO stress and below 3.0 mg L^{-1} indicates that the environment is in a hypoxic condition (Zhi et al., 2023). Among the 1418 rivers analyzed, 110 presented DO ≤3.0 mg L^{-1} (O_2Sat% < 37 %), while 308 rivers presented 3.0 mg L^{-1} < DO ≤5.0 mg L^{-1} (O_2Sat% < 64 %).

The electric conductivity (EC) ranged from 2 to 1731 μS cm^{-1}, with an average of 125 ± 163 μS cm^{-1}. The main source of ions in surface water is the result of chemical weathering of rocks. Carbonate lithotypes have greater susceptibility to chemical over-degradation than silicate lithotypes. Therefore, the type of rock influences the rate of weathering. This natural process is the primary factor responsible for the considerable spatial variation in conductivity observed in river (C.V.: 130 %).

The mean of total alkalinity (TA) was 1.8 ± 3.0 mM, with a maximum of 30.2 mM. The spatial variability (C.V.: 166 %) observed is consistent with the lithological differences present within the basin. Microbasins dominated by carbonate rocks exhibit higher concentrations, particularly in the karst zone to the north. The TA ≥ 1.0 mM in 38 % of the microbasins (544 samples) and 7 % is higher than 6.0 mM (102 samples). Additionally, a strong positive correlation was observed between TA and EC ($\rho = 0.78$, $p < 0.05$). The TA > 3.0 mM ($n = 245$) were identified as outliers, with the majority of these occurring in the karstic region (northern).

The $pH_{measured}$ < $pH_{corrected}$ but the C.V.: 9 % remained the same (Fig. S5 in Supplementary Material). The Mann-Whitney test demonstrated a significantly different ($p < 0.05$). The $pH_{measured}$ *in situ* ranged from 4.130 to 9.210, with an average and standard deviation (SD) of 6.885 ± 0.627. The $pH_{measured}/pH_{corrected}$ was 0.973 ± 0.008 (average ± SD). The $pH_{corrected}$ ranged from 4.372 to 9.368 (7.071 ± 0.613). The 5.132 > $pH_{corrected}$ < 9.210 were identified as outliers (15 samples, ROUT 1 %). These values were located mainly in northern region. The correction of *in situ* pH measurements was carried out to reduce the error generated by the inaccuracy of the parametric probes due to ionic strength (Liu et al., 2020). These efforts are to keep estimates as reliable as possible.

4.3. pCO_2 corrected

Using $pH_{corrected}$ and TA data, CO_2 partial pressure (pCO_2) in rivers and streams was calculated using the carbonate system equilibrium. The results demonstrated a pCO_2 range of 7 to 315,078 μatm with an average of 7491 ± 14,387 μatm (C.V.: 192 %). The error propagation of the pCO_2 showed C.V.: 127 % (from 0.5 to 2120 μatm). Values below 60 μatm occur sporadically and represent <1 % of the analyzed rivers.

The pCO_2 calculation from the carbonate equilibrium is a widely used method in freshwaters, particularly through the pH-TA pair. This is due to the fact that these parameters are easily and frequently measured for monitoring water bodies and managing and studying river basins, both by governmental agencies and research institutions. Moreover, numerous small rivers and streams have low accessibility, which makes it difficult to measure certain parameters *in situ*, even with portable equipment. Consequently, the equilibrium of the carbonate system becomes an important methodology for estimating CO_2 degasification and incorporating small rivers into global carbon balances. This is of particular importance in the context of high-resolution mapping of large river basins. Nevertheless, there is considerable concern about the potential for systematic errors to arise from this application. Consequently, efforts have been made to enhance the accuracy of pCO_2 estimates derived from pH-TA measurements (Abril et al., 2015; Liu et al., 2020; Tang et al., 2023; Wang et al., 2021).

The *in situ* pH and the influence of organic alkalinity are two factors that have been widely discussed and identified as the main factors responsible for systematic errors in pCO_2 calculations using the pair pH-TA. Most rivers have a dominance of carbonate alkaline, and it is widely accepted that TA ~ AlkCarb (HCO_3^- and CO_3^{2-}) in hydrogeochemical studies (Hunt et al., 2011; Wang et al., 2021). However, when it comes to calculating CO_2 concentration, it is important to consider the role of organic alkalinity (OrgAlk = non-carbonate alkalinity, NC-Alk), which includes phosphorus, nitrogen, organic acids, and silicon) should not be neglected (Abril et al., 2015; Wang et al., 2021). This has been particularly demonstrated in acidic organic-rich water (Abril et al., 2015; Hunt et al., 2011; Liu et al., 2020; Wang et al., 2021). Abril et al. (2015) showed that in water with neutral to basic pH and high alkalinity, the carbonate equilibrium produces pCO_2 values consistent with those measured *in situ*. However, acidic pH and TA values (approximately pH < 7 and TA < 1,0 mM) can result in an overestimation of pCO_2 that is up to 300 % higher than the values measured *in situ* (Abril et al., 2015).

Studies indicate that organic acids do not exceed 80 % of dissolved organic carbon (DOC) in molar concentrations determinate by secondary titration (Hunt et al., 2011). Furthermore, the contribution of organic acid anions to alkalinity is not >10 % of their concentrations (pH > 5) (Lozovik, 2005). Consequently, a correction of OrgAlk based on DOC concentration has been proposed and utilized in the literature (Liu et al., 2020). Nevertheless, the authors suggest that the correction be made only if there are direct DOC measurements. Therefore, DOC predictions based on its correlation with DIC are not applied to correct organic alkalinity. Given the inability to apply a correction for OrgAlk was not possible in this study, a correction was applied to the final calculated pCO_2 values.

Tang et al. (2023) developed a model in logarithmic transformation between $pCO_{2calculated}$ with CO2SYS and $pCO_{2measured}$ with the headspace equilibration. The model was applied in this study, and the $pCO_{2corrected}$ ranged from 66 to 20,200 μatm (2191 ± 1791 μatm; C.V.: 82 %). The spatial distribution of the $pCO_{2corrected}$ can be seen in Fig. 1a. The Mann-Whitney test demonstrated a statistically significantly difference between the median values ($p < 0.05$). Following correction, 76 % of rivers and streams (1084 samples) exhibited a $pCO_{2corrected}$ < $pCO_{2calculated}$ (Fig. 1b-d). The $pCO_{2corrected}$ was found to be between 1 and 15 times lower than the $pCO_{2calculated}$. In 334 rivers (representing 24 % of the total number of samples), the $pCO_{2corrected}$ value exceeded the $pCO_{2calculated}$ value by a factor of up to 9. This phenomenon occurs in samples with a higher pH (> 7.0) and a lower alkalinity (< 0.3 mM).

5. Discussion

5.1. Carbonate system equilibrium

Riverine systems are typically supersaturated with CO_2 and act as sources to the atmosphere. About 95 % of the river and streams in Upper São Francisco Basin exhibited CO_2 outgassing processes. So about 5 % of the rivers analysis presented atmospheric CO_2 consumption, specialized sporadically along the Basin. Wen et al. (2021) evaluated about 6700 rivers and streams and found similar resultant, where 95 % had a pCO_2 greater than the atmospheric value.

Lower values in riverine systems could indicate specific dynamics within the drainage basin, such as the removal of CO_2 through photosynthesis or the decrease in pCO_2 caused by natural aeration due to high current velocities, which is common in regions near waterfalls. In contrast, the decomposition of organic matter generally contributes to an increase in CO_2 concentrations due to its release during the degradation process (Tang et al., 2023). Estimates of the influence of different processes on emissions are still scarce. Recently, the processes of CO_2 consumption and release was studied and showed diurnal variation due to metabolic processes with nocturnal emissions about 31 % greater than daytime (Woodrow et al., 2024).

Outliers of pCO_2 (concentration higher than 5870 μatm) are observed in the Upper São Francisco Basin, mainly in karstic region, in

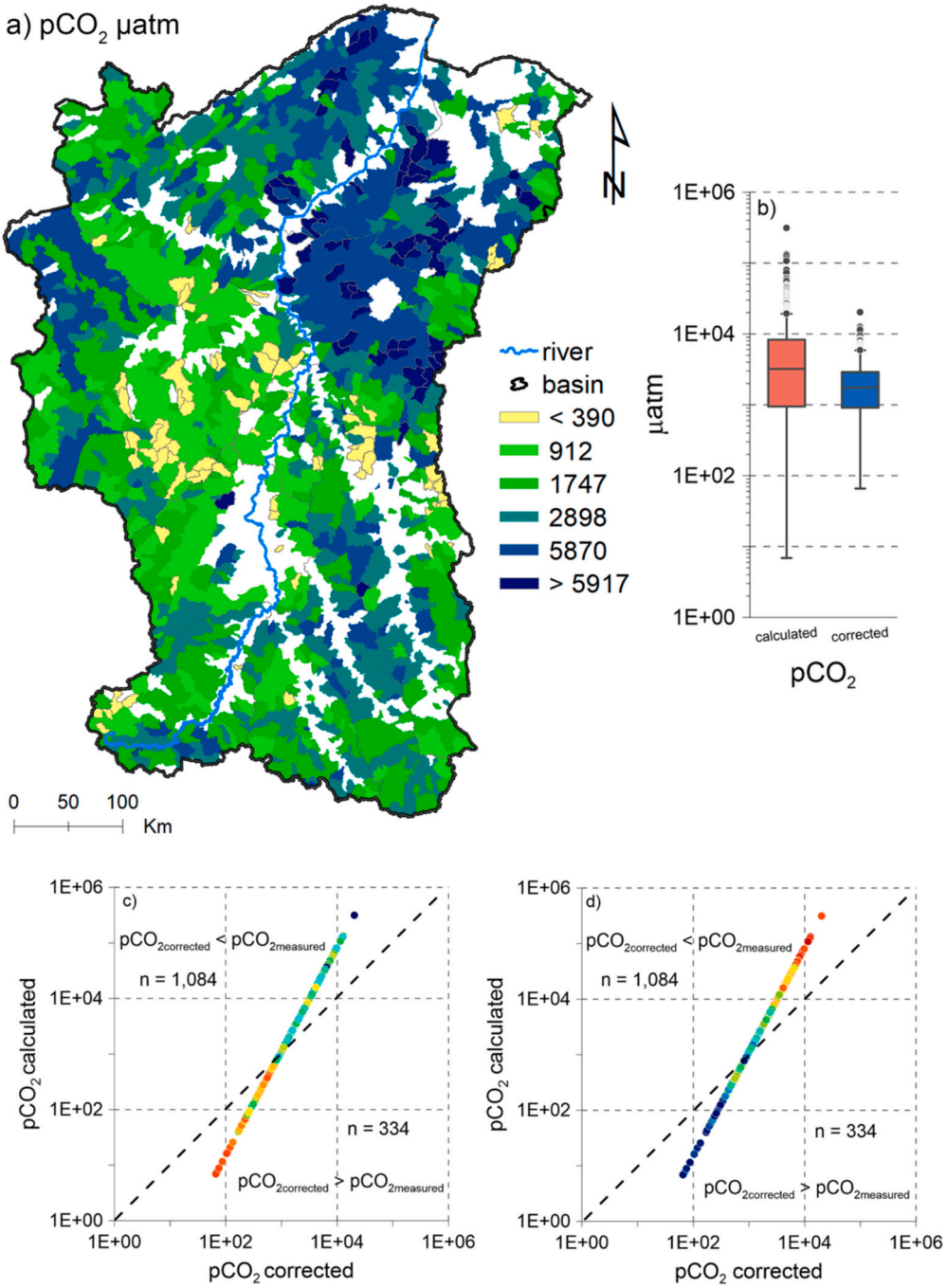

Fig. 1. CO_2 partial pressure in the Upper São Francisco Basin, Brazil: a) spatial distribution (a) of pCO_2 corrected in the river (white color in the map = no data), b) box plot between pCO_2 calculated by pH-TA and pCO_2 corrected by Tang et al. (2023), c) correlation between pCO_2 calculated and pCO_2 corrected with pH values and, d) correlation between pCO_2 calculated and pCO_2 corrected with total alkalinity values.

the northern region. The presence of carbonate lithotypes from the Bambuí Group, mainly dolomites from the Lagoa de Jacaré formation, is evident in these rivers. On the other hand, concentrations lower than the atmosphere (about lower than 390 µatm) are found in the central region of the basin.

The carbonate lithology is highly susceptible to chemical weathering, leading to the release of HCO_3^- ions into the water surface. This process not only enhances dissolved inorganic carbon (DIC) concentrations but also affects the buffering potential of the aquatic ecosystem.

Previous studies also indicate the anthropogenic influence on these rivers, especially from the agriculture (Machado et al., 2024). Nutrient concentration in aquatic environments triggers a series of complex biogeochemical interactions and influences both alkalinity balance and biomass production and respiration/photosynthesis processes, thereby affecting the dynamics of inorganic dissolved carbon.

Additionally, hypoxic condition (as found in about 8 % of the river) are not expected in smaller and shallower rivers and streams. This characteristic that facilitates the entry of light, which favors gas exchange. Deoxygenation is an important process that drives greenhouse gas emissions, in addition to influencing the mobilization of nutrients and toxic metals.

This study did not investigate the sources of carbon directly, but the results suggest an influence of both natural and anthropogenic sources. Land use changes can significantly alter carbon dynamics in rivers and

affect CO_2 degassing processes. One hypothesis is that agricultural activities have been impacting and reshaping carbon dynamics in this region. Furthermore, the observed low pCO_2 values might be attributed to groundwater inputs with low CO_2 concentrations or the presence of oligotrophic conditions during the dry period, both of which require further investigation to fully elucidate the mechanisms driving carbon dynamics in these systems.

While this study employed indirect methods to estimate pCO_2, we recognize the critical role of biological processes in regulating carbon dynamics, which represents an important limitation of this work. Future research should prioritize direct, multiscale approaches to capture the interplay of hydrological, biological, and anthropogenic factors, providing a more comprehensive understanding of carbon dynamics in tropical river systems.

5.2. Physical and chemical control of degassing

5.2.1. Dissipation rates

Gas exchanges at the water-atmosphere interface in aquatic environments are controlled by a multitude of factors, including physical processes (such as turbulence and molecular diffusion), chemical factors (*e.g.*, pH and dissolution constants), and biological aspects such as the production or consumption of the gas (Bade, 2009). The interaction occurring at the water-atmosphere interface is the result of a complex array of biogeochemical processes. These processes drive equilibrium reactions that facilitate mass and energy exchange, resulting in significant material fluxes at a global scale (Allen and Pavelsky, 2018).

In small streams and rivers, turbulence is primarily generated by water flux and bed roughness. The rate of energy dissipation, which is often used as a proxy for near-surface turbulence, assists in the design and understanding of gas exchange in aquatic environments (Ulseth et al., 2019). The turbulence (or energy dissipation) in the liquid phase is one of the most important process that controls the rate of CO_2 gas transfer at the water surface (Borges et al., 2004).

The dissipation rates were investigated, and the results indicated that bed friction ($\varepsilon_s = 0.07 \pm 0.07$ m^3 s^{-2}) is higher than depth-scale form drag ($\varepsilon_d = 0.03 \pm 0.02$ m^3 s^{-2}) in about 87 % of the analyzed rivers. The results were compared with those of Raymond et al. (2012), which explored how ε_d and ε_s vary for average streams across the United States. The findings indicated that ε_d is generally predicted to be higher than ε_s, with the exception for first-order streams.

The rivers in the Upper São Francisco Basin are all low-order streams. Despite the observed differences in size, no correlation was found between the dissipation rates and the area of the microbasins. Positive correlation indicated slope as the primary hydraulic factor controlling turbulence for ε_s ($\rho = 0.85$, $p < 0.05$) and ε_d ($\rho = 0.69$, $p < 0.05$), following by elevation for ε_s ($\rho = 0.80$, $p < 0.05$) and ε_d ($\rho = 0.63$, $p < 0.05$). This outcome serves to reinforce the significance of small, high-elevation rivers, as previously discussed by (Ulseth et al., 2019).

Bed friction turbulence also exhibited a moderate positive correlation with width ($\rho = 0.48$, $p < 0.05$) and depth ($\rho = 0.30$ $p < 0.05$). On the other hand, near-surface turbulence showed a significant positive correlation with velocity ($\rho = 0.60$, $p < 0.05$). Microbasins with low current velocity, as well as shallow depth, tended toward the extremes of pure bed friction.

The roughness of the channel increases turbulence, which in turn increases the rate of reaeration. High turbulence increases the contact surface between the water and the atmosphere, facilitating the exchange of gases. This is particularly important for CO_2 degassing in small rivers and streams where the rate of gas dissipation is strongly influenced by turbulence in the water.

The relationship between dissipation rates (ε_s x ε_d) as a function of slope (S) is showed in Fig. 2. The box plot is shown in Fig. S6 in Supplementary Material.

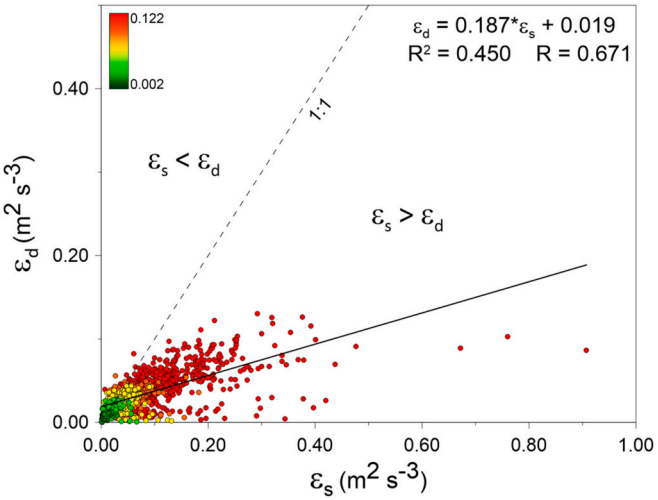

Fig. 2. Relationship between dissipation rates bed friction (ε_s, m^3 s^{-2}) and depth-scale form drag (ε_d, m^3 s^{-2}) as a function of slope (S).

5.2.2. Gas transfer velocity

Gas transfer velocity (k_{CO_2}) constitutes one of the parameters for calculating CO_2 flux at the water-atmosphere interface. This parameter is influenced by both hydrology and the topography of the drainage basin. The estimation of the CO_2 gas transfer rate (k_{CO_2}) is a challenging task, and the associated uncertainties in calculation are considerable. In this study, the ratio and parameterization method with k_{600} was employed.

Thus, an initial review of the various parametrization equations for k_{600} that have been reported in the literature was conducted. Given that wind speed is not a significant parameter in small rivers, equations incorporating these parameters have been removed (Alin et al., 2011). The river hydraulic parameters employed in this study were current velocity (V), depth (D), and slope (S). The equations were preliminary evaluation, resulting in the selection of six for inclusion in this study (see Table 1). The results of the equations were spatialized and compared using a box plot (Fig. 3 and Fig. S7 in Supplementary Material).

The means, standard deviations and variations of the parameterizations in ascending order were, Eq. 5 48 ± 25 (9 to 166) < Eq. 6 49 ± 34 (4 to 234) < Eq. 4. 50 ± 24 (1 to 149) < Eq. 1132 ± 103 (1 to 983) < Eq. 2156 ± 127 (1 to 1258) Eq. 3321 ± 116 (61 to 1090).

Of the six evaluated equations, three employ only variables V and S (eqs. 3, 4, and 5). The coefficient of variation (C.V.) of these equations was found to be the lowest compared to the other parameterizations. In descending order, the Eq. 3 (C.V.: 36 %) < Eq.4 (C.V.: 48 %) < Eq. 5 (C.V.: 52 %). The Kruskal-Wallis test indicated that there was no significant difference between Eqs. 4 and 5. However, both equations exhibited a statistically significant difference in relation to Eq. 3.

In equations Eq. 1 and Eq. 2, depth is incorporated into the functions. It can be observed that depth increases the coefficient of variation, with Eq. 2 (C.V.: 81 %) > Eq. 1 (C.V.: 78 %). Moreover, Eq. 2 is the only equation that employs the Froude number (*Fr*) as a parameter. For the Upper São Francisco Basin, the *Fr* < 1 for all microbasins, indicating laminar flows, which are characteristic of the dry season (base flow), particularly in small rivers and shallow streams.

Eqs. 1 to 5 were obtained from the studies of Raymond et al., 2012. The authors reviewed numerous equations in the literature and proposed parameterizations based on slope and velocity for areas where direct measurements are not feasible or do not necessitate highly accurate estimates. These equations remain a common feature of the literature, with eq. 5 being a particular focus. It has been recommended that equations with the depth term (Eq. 1 and 2) should not be used in larger rivers since the model fails when attempting to scale the hydraulics. Consequently, as most studies apply to large rivers, the use of

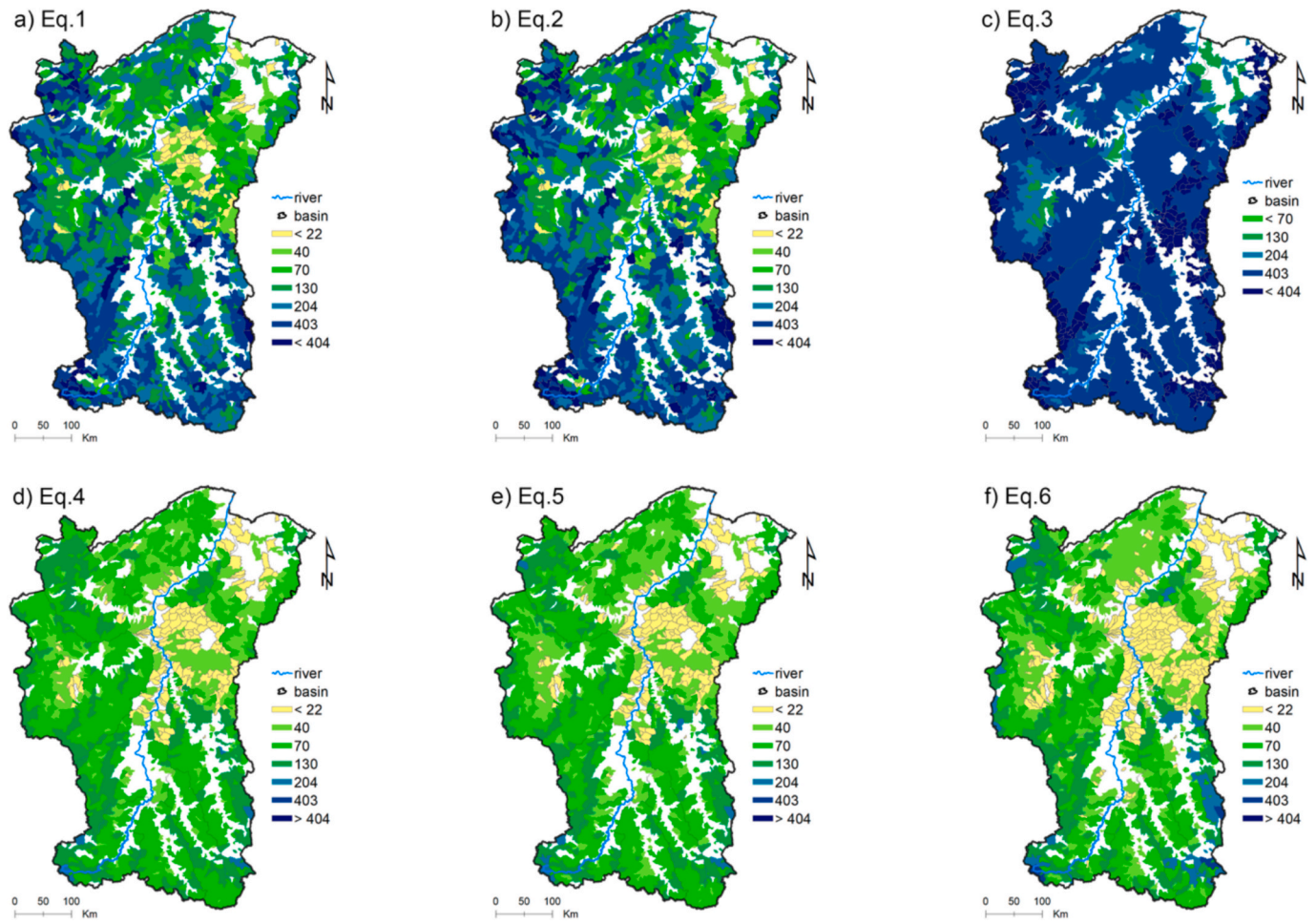

Fig. 3. Spatialization of the k_{600} equations used in the study. a) Eq. 1: k_{600} (m d^{-1}) = $(VS)^{0.89}$ $D^{0.54}$ 5037 (Raymond et al., 2012); b) Eq. 2: k_{600} (m d^{-1}) = 5937 (1–2.54 Fr^2) $(VS^{0.89})$ $D^{0.58}$ (Raymond et al., 2012); c) Eq. 3: k_{600} (m d^{-1}) = 1162 $S^{0.77}$ $V^{0.85}$ (Raymond et al., 2012); d) Eq. 4: k_{600} (m d^{-1}) = $(VS)^{0.76}$ 951.5 (Raymond et al., 2012); e) Eq. 5: k_{600} (m d^{-1}) = *VS* 2841 + 2.02 (Raymond et al., 2012) and f) Eq. 6: ln[k_{600}] (m d^{-1}) = 3.10 + 0.35 ln[εd] (εd < 0.02); ln[k_{600}] (m d^{-1}) = 6.43 + 1.18 ln[εd] (εd > 0.02) (Ulseth et al., 2019). White = no data.

velocity and slope has been more commonly utilized. However, the authors have emphasized the accuracy of these equations for determining the gas transfer velocity in smaller rivers (Raymond et al., 2012).

Eq. 6, proposed by Ulseth et al. (2019) using dissipation energy (ε_d) as a proxy for k_{600} parameterizing, exhibited a coefficient of variation (CV) of 69 % and a statistically significant correlation with Eq. 5. Ulseth et al. (2019) noted that the relationship between k_{600} and geomorphology/hydraulics cannot be generalized for steep-slopes rivers and streams. Empirical models based on slope, current velocity, and depth, while stable for low gradients, may underestimate k_{600} in high-gradient streams. Given the prevalence of high slopes among the evaluated rivers, Eq. 6 was included to potentially improve k_{600} estimation in these steeper systems.

The k_{600} in small rivers ranges from 3 to 70 cm h^{-1} (Li et al., 2019),

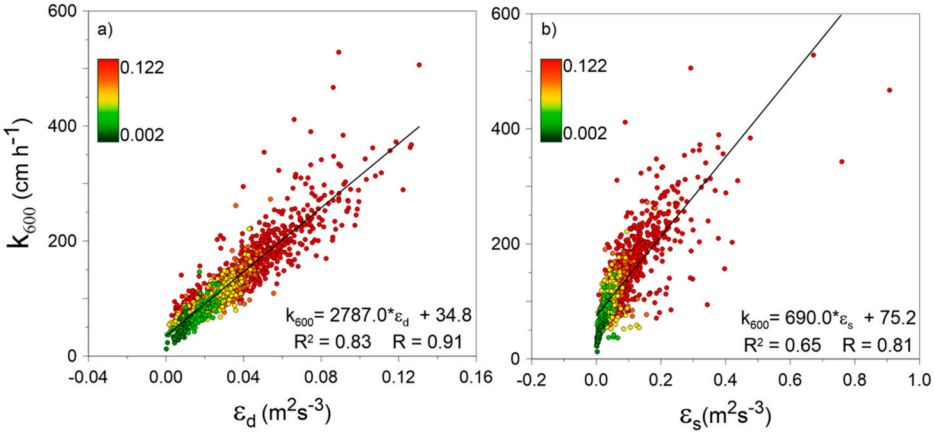

Fig. 4. Correlated between rate of dissipation energy (ε_d and ε_s) the increase in channel slope.

and the global average for fluvial systems is from 8 to 33 cm h^{-1} (Butman and Raymond, 2011; Raymond et al., 2013). Eqs. 4, 5 and 6 generally showed values above the global average for rivers, while eqs. 1, 2 and 3 were above the estimated averages for small rivers.

Thus, eqs. 4, 5 and 6 exhibited low k_{600} values, particularly in the karst region. Conversely, Eq.3 exhibited extremely high values throughout the basin. Eqs. 1 and 2 showed more varied values, with k_{600} higher at the edges of the basins, where the microbasins with the highest elevations, slopes and current velocity are located.

A significant positive correlation was observed between the k_{600} and the rate of dissipation energy (ε_d and ε_s). The Fig. 4 illustrates that the increase in these parameters is linearly correlated with the increase in channel slope.

The k_{CO_2} value was finally calculated using each of the six parameterizations. The maximum values observed in all parameterizations exceed the global average value. The k_{CO_2} can exhibit a wide variation in small rivers ranging from 1 to 100 cm h^{-1} (Li et al., 2020). The values of Eqs. 4 and 5 are approximately twice the average value. In contrast, eq. 6 exceeds this by a factor of three. It is possible for Eqs. 1, 2, and 3 to reach values that are approximately 11, 10 to 14 times greater, respectively.

The absence of *in situ* measurements of the gas rate in the region makes it challenging to ascertain the optimal parameterization for the Upper São Francisco Basin. The high spatial variability in the values is due to the great diversity in terms of morphology, fluxes, and environmental characteristics of the small rivers. In order to minimize the potential for underestimation or overestimation of values, the fluxes were calculated using each of the equations. The estimates were derived from the mean values.

5.3. Estimates of CO_2 emissions

Among the rivers and streams analyzed, 5 % of them exhibited negative fluxes (75 rivers), which indicates that they consume CO_2. A comparison of the flow values obtained by each k_{600} equation is shown in Fig. S8 in Supplementary Material. For the purpose of fluxes estimation, only samples with a pH $\geq$ 6 were considered. The average FCO_2 was 1.9 $\pm$ 1.9 mol m^{-2} d^{-1} for 1263 samples (25th = 0.6; 50th = 1.5 and 75th =2.7 mol m^{-2} d^{-1}) and C.V.: 98 % (see spatial distribution in Fig. 5).

Estimate of CO_2 fluxes at the water-atmosphere interface was calculated for the entire Upper São Francisco Basin. The median and the interquartile values (25th and 75th) have been used to generate an estimate and a range of CO_2 emissions. The results were then compared with those obtained for other basins.

The findings indicate that the Upper São Francisco Basin contributes approximately 1.52 Pg C yr^{-1}, with a 95 % confidence interval from 1.40 to 1.64 Pg C yr^{-1}. The range of CO_2 emissions to the atmosphere is estimated to be between 0.65 and 2.72 Pg C yr^{-1}. These values are comparable to those of larger basins. See Table S2 (Supplementary Material) for more comparisons.

CO_2 flux estimations for river systems have been conducted in various regions. For example, emissions in the Amazon River Basin were estimated at ~0.47 Pg C yr^{-1} (Richey et al., 2002). Butman and Raymond (2011) assessed U.S. streams and rivers, estimating ~0.1 Pg C yr^{-1}

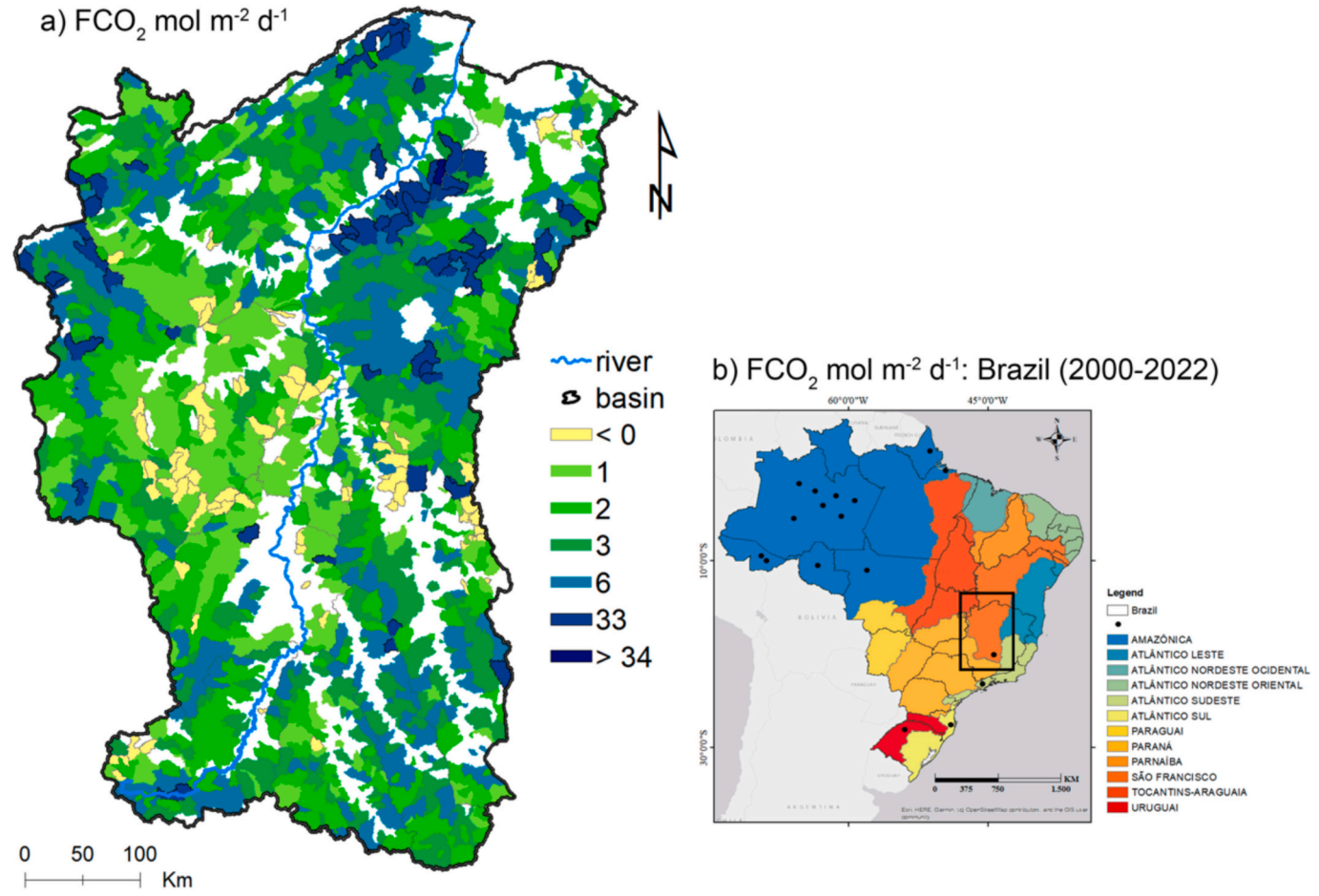

Fig. 5. a) Spatial distribution of the CO_2 fluxes at the water-atmosphere interface in Upper São Francisco Basin, Brazil; White = no data. b) Location of the study area in Brazil. The colors represent the hydrographic regions of Brazil. The black dots represent the locations that have FCO_2 studies between the years 2000–2022 (Machado et al., 2023).

and extrapolating to ~0.5 Pg C yr^{-1}, for temperate rivers between 25° and 50° N. African rivers were analyzed by Borges et al. (2015), who reported fluxes ranging from 0.27 to 0.37 Pg C yr^{-1}. Global studies suggest riverine CO_2 emissions from 0.20 to 2.20 Pg C yr^{-1} (Aufdenkampe et al., 2011; Cole et al., 2007; Raymond et al., 2013; Tang et al., 2023). However, many global estimates are based on fluxes from large temperate rivers and the Amazon due to limited data from tropical zones.

Gómez-Gener et al. (2021) utilized a compilation of global river data and demonstrated that, mainly due to photosynthesis, nighttime CO_2 emissions are on average 27 % higher than estimates based solely on daytime observations, as conducted in this study. Additionally, the study demonstrated that rivers draining temperate biomes exhibited greater internal variability when compared to rivers in tropical/subtropical and boreal systems. Liu et al. (2022) estimated that CO_2 emissions are higher in tropical rivers than in temperate and arctic rivers. However, they demonstrated that the monthly variability of CO_2 emissions is lower in tropical and southern temperate rivers (C.V.: 4 %) compared to northern boreal and temperate rivers (C.V.: 25 to 37 %). The authors further suggest that tropical rivers contribute 57 % of CO_2 emissions from river systems, while temperate zones account for 30 % and the arctic for 13 %.

In addition to the influence of the climate zone, local characteristics such as lithology and land use can also influence the dynamics of degassing. In the Upper São Francisco Basin, the karst region had the highest level of CO_2 emissions. Liu and Han (2021) observed CO_2 emissions in the rivers of the Xijiang River Basin, China, and concluded that the spatial distribution was primarily controlled by lithology rather than anthropogenic inputs, with higher emissions in silicate terrains compared to karst terrains. This was attributed to elevated pH, which increases buffering capacity and reduces pCO_2 from DIC (low CO_2). Conversely, Li et al. (2023) studied karst rivers in the Nanming River basin and found high potential CO_2 fluxes. They suggested that urban development could increase pCO_2 in karst rivers, leading to increased CO_2 fluxes.

Urbanization, through sewage and effluent discharge, as well as agricultural practices, can increase nutrient and carbon loads in surface waters, affecting biogeochemical processing and disrupting the balance between CO_2 production and consumption (Jin et al., 2018). This process is particularly important in karst regions, which are sensitive to minimal environmental changes.

Lima et al. (2022) assessed the anthropogenic impacts on the hydrological cycle of the São Francisco River Basin between 1985 and 2015 and found that land use and land cover changes have intensified over the years, mainly driven by agriculture. The MSF region experienced concentrated agricultural expansion, with agricultural production increasing up to sixfold between 1995 and 2012, driven by large-scale agriculture (especially soybean cultivation). By 2013, approximately 1400 irrigation pivots were observed in the region (Lima et al., 2022). The results of this study suggest the hypothesis that the high values in the karst zone are a response to anthropogenic influence. We emphasize the importance of further research in basins with a high level of anthropogenic influence, agriculture and urbanization, especially in the karst zone.

6. Conclusion

While tropical rivers are recognized as significant sources of atmospheric CO_2, estimates for these ecosystems, particularly small rivers and streams, remain scarce. This knowledge gap motivated the present study. The challenges associated with estimating CO_2 degassing in riverine environments have been previously discussed.

One of the challenges is the accuracy of the pCO_2 calculations. Following correction, 76 % of the rivers analyzed exhibited $pCO_{2corrected}$ up to 15 times lower than $pCO_{2calculated}$ from the equilibrium of the carbonate system using pH-TA parameters. The mean $pCO_{2corrected}$ value was 2191 ± 1791 μatm (from 66 to 20,200 μatm). Approximately 95 % of the rivers and streams in the Upper São Francisco Basin exhibited CO_2 outgassing processes, with fluxes ranging from 0.65 to 2.72 Pg C yr^{-1}. It was estimated that the Upper São Francisco Basin contributes about 1.52 Pg C yr^{-1}, with a 95 % confidence interval of 1.40 to 1.64 Pg C yr^{-1}.

To calculate the fluxes, a series of k_{600} equations were evaluated. The high-resolution mapping employed in this study enables the observation of spatial variations in k_{600}. The results indicate that there are statistically significant differences between the equations. The absence of *in situ* data renders it challenging to ascertain the most suitable equation for application. Nevertheless, the rate of dissipation due to bed roughness and slope may serve as promising proxies for estimating k_{600} in small rivers and streams. Of the 1418 rivers analyzed, 87 % exhibited a greater influence from the rate of dissipation due to bed roughness than the rate of dissipation due drag scale. This factor renders small rivers and streams relevant to the carbon balance in river systems, as the roughness favors an increase in the rate of reaeration.

The findings of this study indicate that the carbon dynamics in the rivers of the Upper São Francisco basin are undergoing alteration as a consequence of anthropogenic influence, particularly in those rivers that drain the karst zone. Further investigation is required to elucidate the impact of land use changes on CO_2 degassing in the region.

This study provides the first estimate of CO_2 fluxes for the Upper São Francisco Basin. By producing a robust estimate, this work offers valuable insights into the study area and contributes to addressing the data gap in tropical regions. We emphasize the need for future direct investigations to obtain more accurate estimates and enhance our understanding of small rivers' role in the global carbon cycle.

CRediT authorship contribution statement

Daniela Vasconcelos Machado: Writing – original draft, Methodology, Investigation, Conceptualization. **Eduardo Duarte Marques:** Writing – review & editing, Software, Resources, Data curation. **Andréa da Consolação de Oliveira Carvalho:** Writing – review & editing. **Eduardo Paim Viglio:** Resources, Data curation. **Everton Assunção Martins dos Santos:** Software, Data curation. **Rozane Valente Marins:** Writing – review & editing. **Gerson Cardoso da Silva Júnior:** Writing – review & editing. **Emmanoel Vieira Silva-Filho:** Writing – review & editing, Supervision.

Declaration of competing interest

The authors declare that they have no known competing financial interests or personal relationships that could have appeared to influence the work reported in this paper.

Acknowledgments

This study was funded by institutions Carlos Chagas Filho Foundation of Research Support of the State of Rio de Janeiro (FAPERJ) – E-26/200.695/2021 (262375). CAPES - Coordenação de Aperfeiçoamento de Pessoal de Nível Superior - Finance Code 001. This study is an output of the INCT Continent-Ocean Materials Transfer (INCT-TMCOcean) supported by the Conselho Nacional de Desenvolvimento Científico e Tecnológico - CNPq, Proc. No. 405.765/2022–3.

Appendix A. Supplementary data

Supplementary data to this article can be found online at https://doi.org/10.1016/j.scitotenv.2025.179015.

Data availability

Data will be made available on request.

References

Abril, G., Bouillon, S., Darchambeau, F., Teodoru, C.R., Marwick, T.R., Tamooh, F., Ochieng Omengo, F., Geeraert, N., Deirmendjian, L., Polsenaere, P., Borges, A.V., 2015. Technical note: large overestimation of pCO2 calculated from pH and alkalinity in acidic, organic-rich freshwaters. Biogeosciences 12, 67–78. https://doi.org/10.5194/bg-12-67-2015.

Alin, S.R., Rasera, M. de F.F.L., Salimon, C.I., Richey, J.E., Holtgrieve, G.W., Krusche, A. V., Snidvongs, A., 2011. Physical controls on carbon dioxide transfer velocity and flux in low-gradient river systems and implications for regional carbon budgets. J. Geophys. Res. 116, G01009. https://doi.org/10.1029/2010JG001398.

Allen, G.H., Pavelsky, T.M., 2018. Global extent of rivers and streams. Science 361, 585–588. https://doi.org/10.1126/science.aat0636.

Aufdenkampe, A.K., Mayorga, E., Raymond, P.A., Melack, J.M., Doney, S.C., Alin, S.R., Aalto, R.E., Yoo, K., 2011. Riverine coupling of biogeochemical cycles between land, oceans, and atmosphere. Front. Ecol. Environ. 9, 53–60. https://doi.org/10.1890/100014.

Bade, D.L., 2009. Gas Exchange at the Air–Water Interface, in: Encyclopedia of Inland Waters. Elsevier, pp. 70–78. doi:https://doi.org/10.1016/B978-012370626-3.00213-1.

Borges, A.V., Vanderborght, J.-P., Schiettecatte, L.-S., Gazeau, F., Ferrón-Smith, S., Delille, B., Frankignoulle, M., 2004. Variability of the gas transfer velocity of CO2 in a macrotidal estuary (the Scheldt). Estuaries 27, 593–603. https://doi.org/10.1007/BF02907647.

Borges, A.V., Darchambeau, F., Teodoru, C.R., Marwick, T.R., Tamooh, F., Geeraert, N., Omengo, F.O., Guérin, F., Lambert, T., Morana, C., Okuku, E., Bouillon, S., 2015. Globally significant greenhouse-gas emissions from African inland waters. Nat. Geosci. 8, 637–642. https://doi.org/10.1038/ngeo2486.

Butman, D., Raymond, P.A., 2011. Significant efflux of carbon dioxide from streams and rivers in the United States. Nat. Geosci. 4, 839–842. https://doi.org/10.1038/ngeo1294.

Canadell, J. G., Monteiro, P. M. S., Costa, M. H., Cotrim da Cunha, L., Cox, P. M., Eliseev, A. V., Henson, S., Ishii, M., Jaccard, S., Koven, C., Lohila, A., Patra, P. K., Piao, S., Rogelj, J., Syampungani, S., Zaehle, S., and Zickfeld, K.: Global Carbon and Other Biogeochemical Cycles and Feedbacks, in: Climate Change 2021: The Physical Science Basis, Contribution of Working Group I to the Sixth Assessment Report of the Intergovernmental Panel on Climate Change, edited by: Masson-Delmotte, V., Zhai, P., Pirani, A., Connors, S. L., Péan, C., Berger, S., Caud, N., Chen, Y., Goldfarb, L., Gomis, M. I., Huang, M., Leitzell, K., Lonnoy, E., Matthews, J. B. R., Maycock, T. K., Waterfield, T., Yelekçi, O., Yu, R., and Zhou, B., Cambridge University Press, Cambridge, United Kingdom and New York, NY, USA, 673–816, doi:https://doi.org/10.1017/9781009157896.007, 2021.

Cole, J.J., Prairie, Y.T., Caraco, N.F., McDowell, W.H., Tranvik, L.J., Striegl, R.G., Duarte, C.M., Kortelainen, P., Downing, J.A., Middelburg, J.J., Melack, J., 2007. Plumbing the global carbon cycle: integrating inland waters into the terrestrial carbon budget. Ecosystems 10, 172–185. https://doi.org/10.1007/s10021-006-9013-8.

Dickson, A.G., 1990. Standard potential of the reaction: AgCl(s) +iH, (g) = ag(s) + HCl (aq), and and the standard acidity constant of the ion HSOh in synthetic sea water from 273.15 to 318.15 K. doi:https://doi.org/10.1016/0021-9614(90)90074-Z.

FJP, 2019. Produto interno bruto dos municípios de Minas Gerais: ano de referência 2017 / Fundação João Pinheiro. FJP, Diretoria de Estatística e Informações. – Belo Horizonte, p. 2019 (ISSN 2595-6132).

Gómez-Gener, L., Rocher-Ros, G., Battin, T., Cohen, M.J., Dalmagro, H.J., Dinsmore, K.J., Drake, T.W., Duvert, C., Enrich-Prast, A., Horgby, Å., Johnson, M.S., Kirk, L., Machado-Silva, F., Marzolf, N.S., McDowell, M.J., McDowell, W.H., Miettinen, H., Ojala, A.K., Peter, H., Pumpanen, J., Ran, L., Riveros-Iregui, D.A., Santos, I.R., Six, J., Stanley, E.H., Wallin, M.B., White, S.A., Sponseller, R.A., 2021. Global carbon dioxide efflux from rivers enhanced by high nocturnal emissions. Nat. Geosci. 14, 289–294. https://doi.org/10.1038/s41561-021-00722-3.

Hunt, C.W., Salisbury, J.E., Vandemark, D., 2011. Contribution of non-carbonate anions to total alkalinity and overestimation of pCO2 in New England and New Brunswick rivers. Biogeosciences 8, 3069–3076. https://doi.org/10.5194/bg-8-3069-2011.

Jähne, B., Münnich, K.O., Bösinger, R., Dutzi, A., Huber, W., Libner, P., 1987. On the parameters influencing air-water gas exchange. J. Geophys. Res. 92, 1937. https://doi.org/10.1029/JC092iC02p01937.

Jin, H., Yoon, T.K., Begum, M.S., Lee, E.-J., Oh, N.-H., Kang, N., Park, J.-H., 2018. Longitudinal discontinuities in riverine greenhouse gas dynamics generated by dams and urban wastewater. Biogeosciences 15, 6349–6369. https://doi.org/10.5194/bg-15-6349-2018.

Joshi, P., Siddaiah, N.S., 2021. Carbon dioxide dynamics of Bhalswa Lake: a human-impacted urban wetland of Delhi, India. Environ. Dev. Sustain. 23, 18116–18142. https://doi.org/10.1007/s10668-021-01430-z.

Keller, P.S., Catalán, N., von Schiller, D., Grossart, H.-P., Koschorreck, M., Obrador, B., Frassl, M.A., Karakaya, N., Barros, N., Howitt, J.A., Mendoza-Lera, C., Pastor, A., Flaim, G., Aben, R., Riis, T., Arce, M.I., Onandia, G., Paranaíba, J.R., Linkhorst, A., del Campo, R., Amado, A.M., Cauvy-Fraunié, S., Brothers, S., Condon, J., Mendonça, R.F., Reverey, F., Rõõm, E.-I., Datry, T., Roland, F., Laas, A., Obertegger, U., Park, J.-H., Wang, H., Kosten, S., Gómez, R., Feijoó, C., Elosegi, A., Sánchez-Montoya, M.M., Finlayson, C.M., Melita, M., Oliveira Junior, E.S., Muniz, C. C., Gómez-Gener, L., Leigh, C., Zhang, Q., Marcé, R., 2020. Global CO2 emissions from dry inland waters share common drivers across ecosystems. Nat. Commun. 11, 2126. https://doi.org/10.1038/s41467-020-15929-y.

Lee, K., Millero, F.J., Byrne, R.H., Feely, R.A., Wanninkhof, R., 2000. The recommended dissociation constants for carbonic acid in seawater. Geophys. Res. Lett. 27, 229–232. https://doi.org/10.1029/1999GL002345.

Leopold, L.B., Maddock, T., 1953. The Hydraulic Geometry of Stream Channels and some Physiographic Implications. Government Printing Office, U.S, p. 57.

Lewis, E., Wallace, D., Allison, L.J., 1998. Program developed for CO2 system calculations: oak ridge TN. Oak Ridge National Laboratory Environmental Sciences Division. https://doi.org/10.2172/639712.

Li, K., Cao, X., Zhou, S., Li, L., 2023. Spatial and temporal distribution characteristics of pCO2 and CO2 evasion in karst rivers under the influence of urbanization. Environ. Sci. Pollut. Res. 30, 53920–53937. https://doi.org/10.1007/s11356-023-26144-9.

Li, S., Ni, M., Mao, R., Bush, R.T., 2018. Riverine CO2 supersaturation and outgassing in a subtropical monsoonal mountainous area (three gorges reservoir region) of China. J. Hydrol. 558, 460–469. https://doi.org/10.1016/j.jhydrol.2018.01.057.

Li, S., Mao, R., Ma, Y., Sarma, V.V.S.S., 2019. Gas transfer velocities of CO2 in subtropical monsoonal climate streams and small rivers. Biogeosciences 16, 681–693. https://doi.org/10.5194/bg-16-681-2019.

Li, S., Luo, J., Wu, D., Jun Y., Xu, 2020. Carbon and nutrients as indictors of daily fluctuations of pCO2 and CO2 flux in a river draining a rapidly urbanizing area. Ecol. Indic. 109, 105821. https://doi.org/10.1016/j.ecolind.2019.105821.

Lima, C.E.S., Da Silva, M.V.M., Rocha, S.M.G., Silveira, C.D.S., 2022. Anthropic changes in land use and land cover and their impacts on the hydrological variables of the São Francisco River basin, Brazil. Sustainability 14, 12176. https://doi.org/10.3390/su141912176.

Liss, P.S., Slater, P.G., 1974. Flux of gases across the Air-Sea Interface. Nature 247, 181–184. https://doi.org/10.1038/247181a0.

Liu, J., Han, G., 2021. Controlling factors of riverine CO2 partial pressure and CO2 outgassing in a large karst river under base flow condition. J. Hydrol. 593, 125638. https://doi.org/10.1016/j.jhydrol.2020.125638.

Liu, S., Butman, D.E., Raymond, P.A., 2020. Evaluating CO2 calculation error from organic alkalinity and pH measurement error in low ionic strength freshwaters. Limnology & Ocean Methods 18, 606–622. https://doi.org/10.1002/lom3.10388.

Liu, S., Kuhn, C., Amatulli, G., Aho, K., Butman, D.E., Allen, G.H., Lin, P., Pan, M., Yamazaki, D., Brinkerhoff, C., Gleason, C., Xia, X., Raymond, P.A., 2022. The importance of hydrology in routing terrestrial carbon to the atmosphere via global streams and rivers. Proc. Natl. Acad. Sci. USA 119, e2106322119. https://doi.org/10.1073/pnas.2106322119.

Lozovik, P.A., 2005. Contribution of organic acid anions to the alkalinity of natural humic water. J. Anal. Chem. 60, 1000–1004. https://doi.org/10.1007/s10809-005-0226-3.

Machado, D.V., Silva Júnior, G.C.D., Marques, E.D., Silva-Filho, E.V., 2023. CO2 fluxes at the water-atmosphere interface in fluvial environments: an overview of studies in Brazilian rivers. Rev. ambiente água 18, 1–15. https://doi.org/10.4136/ambi-agua.2921.

Machado, D.V., Marques, E.D., Viglio, E.P., Dos Santos, E.A.M., Amarante, R.T., Da Silva Júnior, G.C., Silva-Filho, E.V., 2024. High-resolution mapping and multivariate technique (factor analysis) to support hydrogeochemical analysis and identification of surface water contamination. J. Geochem. Explor. 263, 107495. https://doi.org/10.1016/j.gexplo.2024.107495.

Marques, E.D., Castro, C.C., De Assis Barros, R., Lombello, J.C., De Souza Marinho, M., Araújo, J.C.S., Santos, E.A.M., 2023. Geochemical mapping by stream sediments of the NW portion of Quadrilátero Ferrífero, Brazil: application of the exploratory data analysis (EDA) and a proposal for generation of new gold targets in Pitangui gold district. J. Geochem. Explor. 250, 107232. https://doi.org/10.1016/j.gexplo.2023.107232.

Marx, A., Dusek, J., Jankovec, J., Sanda, M., Vogel, T., van Geldern, R., Hartmann, J., Barth, J.A.C., 2017. A review of CO2 and associated carbon dynamics in headwater streams: a global perspective: carbon dioxide in headwater streams. Rev. Geophys. 55, 560–585. https://doi.org/10.1002/2016RG000547.

Millero, F.J., 1979. The Thermodynamics of the Carbonate System in Seawater.

Millero, F.J., 1995. Thermodynamics of the carbon dioxide system in the oceans. Geochim. Cosmochim. Acta 59, 661–677. https://doi.org/10.1016/0016-7037(94)00354-O.

Moog, D., Jirka, G., 1999. Stream Reaeration in Nonuniform Flow: Macroroughness Enhancement.

Neal, C., House, W., Down, K., 1998. An assessment of excess carbon dioxide partial pressures in natural waters based on pH and alkalinity measurements. Sci. Total Environ. 210–211, 173–185. https://doi.org/10.1016/S0048-9697(98)00011-4.

Orr, J.C., Epitalon, J.-M., Dickson, A.G., Gattuso, J.-P., 2018. Routine uncertainty propagation for the marine carbon dioxide system. Mar. Chem. 207, 84–107. https://doi.org/10.1016/j.marchem.2018.10.006.

Parkhurst and Appelo, 1999. User's guide to PHREEQC (Version 2): A computer program for speciation, batch-reaction, one-dimensional transport, and inverse geochemical calculations. doi:https://doi.org/10.3133/wri994259.

Quick, A.M., Reeder, W.J., Farrell, T.B., Tonina, D., Feris, K.P., Benner, S.G., 2019. Nitrous oxide from streams and rivers: a review of primary biogeochemical pathways and environmental variables. Earth Sci. Rev. 191, 224–262. https://doi.org/10.1016/j.earscirev.2019.02.021.

R Core Team, 2022. _R: A Language and Environment for Statistical Computing_. R Foundation for Statistical Computing, Vienna, Austria.

Ran, L., Lu, X.X., Liu, S., 2017. Dynamics of riverine CO2 in the Yangtze River fluvial network and their implications for carbon evasion. Biogeosciences 14, 2183–2198. https://doi.org/10.5194/bg-14-2183-2017.

Raymond, P.A., Zappa, C.J., Butman, D., Bott, T.L., Potter, J., Mulholland, P., Laursen, A. E., McDowell, W.H., Newbold, D., 2012. Scaling the gas transfer velocity and hydraulic geometry in streams and small rivers: gas transfer velocity and hydraulic geometry. Limnol. Oceanogr. 2, 41–53. https://doi.org/10.1215/21573689-1597669.

Raymond, P.A., Hartmann, J., Lauerwald, R., Sobek, S., McDonald, C., Hoover, M., Butman, D., Striegl, R., Mayorga, E., Humborg, C., Kortelainen, P., Dürr, H., Meybeck, M., Ciais, P., Guth, P., 2013. Global carbon dioxide emissions from inland waters. Nature 503, 355–359. https://doi.org/10.1038/nature12760.

Richey, J.E., Melack, J.M., Aufdenkampe, A.K., Ballester, V.M., Hess, L.L., 2002. Outgassing from Amazonian rivers and wetlands as a large tropical source of atmospheric CO2. Nature 416, 617–620. https://doi.org/10.1038/416617a.

Robbins, L.L., Hansen, M.E., Kleypas, J.A., Meylan, S.C., 2010. CO2calc—A User-Friendly Seawater Carbon Calculator for Windows, Max OS X, and iOS (iPhone) (Open-File Report), Open-File Report. U.S. Geological Survey, Open-File Report 2010–1280.).

Rockström, J., Steffen, W., Noone, K., Persson, Å., Chapin, F.S., Lambin, E.F., Lenton, T. M., Scheffer, M., Folke, C., Schellnhuber, H.J., Nykvist, B., de Wit, C.A., Hughes, T., van der Leeuw, S., Rodhe, H., Sörlin, S., Snyder, P.K., Costanza, R., Svedin, U., Falkenmark, M., Karlberg, L., Corell, R.W., Fabry, V.J., Hansen, J., Walker, B., Liverman, D., Richardson, K., Crutzen, P., Foley, J.A., 2009. A safe operating space for humanity. Nature 461, 472–475. https://doi.org/10.1038/461472a.

RStudio Team, 2022. RStudio: Integrated Development for R. RStudio, Inc., Boston, MA. URL http://www.rstudio.com/.

Tang, W., Xu, Y.J., Ni, M., Li, S., 2023. Land use and hydrological factors control concentrations and diffusive fluxes of riverine dissolved carbon dioxide and methane in low-order streams. Water Res. 231, 119615. https://doi.org/10.1016/j.watres.2023.119615.

Tucci, C.E.M., 2001. Hidrologia: Ciência e Aplicação, 2nd ed. ABRH, Porto Alegre, UFRGS.

Ulseth, A.J., Hall, R.O., Boix Canadell, M., Madinger, H.L., Niayifar, A., Battin, T.J., 2019. Distinct air–water gas exchange regimes in low- and high-energy streams. Nat. Geosci. 12, 259–263. https://doi.org/10.1038/s41561-019-0324-8.

Wang, J., Wang, X., Liu, T., Yuan, X., Chen, H., He, Y., Wu, S., Yuan, Z., Li, H., Que, Z., Yu, L., Zhang, Y., 2021. pCO2 and CO2 evasion from two small suburban rivers: implications of the watershed urbanization process. Sci. Total Environ. 788, 147787. https://doi.org/10.1016/j.scitotenv.2021.147787.

Wang-Erlandsson, L., Tobian, A., van der Ent, et al., 2022. A planetary boundary for green water. Nat Rev Earth Environ 3, 380–392. https://doi.org/10.1038/s43017-022-00287-8.

Wanninkhof, R., 1992. Relationship between wind speed and gas exchange over the ocean. J. Geophys. Res. 97, 7373–7382. https://doi.org/10.1029/92JC00188.

Weiss, R.F., 1974. Carbon dioxide in water and seawater: the solubility of a non-ideal gas. Mar. Chem. 2, 203–215. https://doi.org/10.1016/0304-4203(74)90015-2.

Wen, Z., Shang, Y., Lyu, L., Li, S., Tao, H., Song, K., 2021. A review of quantifying pCO2 in inland waters with a global perspective: challenges and prospects of implementing remote sensing technology. Remote Sens. 13, 4916. https://doi.org/10.3390/rs13234916.

Woodrow, R.L., White, S.A., Conrad, S.R., Wadnerkar, P.D., Rocher-Ros, G., Sanders, C. J., Holloway, C.J., Santos, I.R., 2024. Enhanced stream greenhouse gas emissions at night and during flood events. Limnol Oceanogr letters lol2.10374. doi:https://doi.org/10.1002/lol2.10374.

Zappa, C.J., McGillis, W.R., Raymond, P.A., Edson, J.B., Hintsa, E.J., Zemmelink, H.J., Dacey, J.W.H., Ho, D.T., 2007. Environmental turbulent mixing controls on air-water gas exchange in marine and aquatic systems. Geophys. Res. Lett. 34, L10601. https://doi.org/10.1029/2006GL028790.

Zhi, W., Klingler, C., Liu, J., Li, L., 2023. Widespread deoxygenation in warming rivers. Nat. Clim. Chang. 13, 1105–1113. https://doi.org/10.1038/s41558-023-01793-3.